

# Transient isotopic labeling studies using $^{12}\text{CH}_4/^{13}\text{CH}_4$ over alkali-promoted molybdate catalysts in the oxidative coupling of methane

S.A. Driscoll, D.K. Gardner and U.S. Ozkan <sup>1</sup>

*Department of Chemical Engineering, The Ohio State University,  
Columbus, OH 43210, USA*

Received 13 September 1993; accepted 11 January 1994

The methane coupling reaction was investigated over  $\text{MnMoO}_4$  and alkali (Li, Na, K)-promoted  $\text{MnMoO}_4$  at 700°C using  $^{12}\text{CH}_4/^{13}\text{CH}_4$  transient isotopic labeling experiments under steady-state reaction conditions. The variations observed in the surface residence times of  $\text{CH}_4$ , CO, and  $\text{CO}_2$ , ethane and ethylene were used to help explain selectivity differences previously reported in the oxidative coupling of methane over alkali-promoted molybdate catalysts.

**Keywords:** molybdate; methane coupling; isotopic labeling; alkali promoter

## 1. Introduction

Methane oxidative coupling has been a much investigated area in recent years. The initial impetus was provided by Keller and Bhasin [2], whose early research efforts indicated that the selective formation of higher hydrocarbons was possible by separating the catalytic reduction and oxidation steps through cyclic feed operation. Additional research into oxidative coupling of methane by Lunsford and co-workers [3] indicated co-feed operation was also possible, and suggested that the coupling reaction occurs between methyl radicals in the gas phase. Their work was supported by the detection of gas-phase radicals which were formed through hydrogen abstraction on the catalyst surface [3–5]. Deuterium-labeled methane has been used to examine the kinetic isotope effect, supporting the theory that hydrogen abstraction is the rate determining step [6–10]. A number of investigations have since utilized isotopically labeled gases to investigate the reaction and the reaction mechanism [11–21]. These investigations have used labeled oxygen or  $^{13}\text{C}$  labeled methane in the feed gas, examining the reaction under steady-state conditions through an abrupt change from the unlabeled to labeled reactant. One of the bene-

<sup>1</sup> To whom correspondence should be addressed.

fits of using isotopically labeled reactants under steady-state reaction conditions is that component concentrations remain unchanged, so the isotopic yields can be determined by monitoring the molecular ion fragments for the labeled and unlabeled species of each reactant or product. The transients provide information about the relative lifetimes of surface species, or in the case of oxygen, the importance of lattice oxygen versus adsorbed or gas-phase oxygen.

Our work has recently focused on the use of alkali promoters with a simple molybdate catalyst,  $\text{MnMoO}_4$ , for the oxidative coupling reaction. We have examined these catalysts both at equal conversion levels and at equal residence times. In our studies, we have found that the addition of alkali promoters to  $\text{MnMoO}_4$  catalyst increases the catalytic activity at equal residence times, and changes the product distribution in favor of partial oxidation products. The addition of potassium was found to produce the most significant increase in  $\text{C}_2$  selectivity [1]. In studies using isotopically labeled oxygen, we determined that the potassium-promoted  $\text{MnMoO}_4$  catalyst interacts with oxygen in a significantly different manner than the other catalysts investigated, both during steady-state methane coupling reaction and during oxygen exchange in the absence of methane [11]. In this paper, we present the results of experiments using the same isotopic transient technique with  $^{13}\text{C}$ -labeled methane.

## 2. Experimental

Manganese molybdate catalyst was prepared by a precipitation reaction, adding a solution of ammonium heptamolybdate drop-wise to a heated manganese chloride solution at  $80^\circ\text{C}$ , maintaining the pH at a value of 6.0. The resulting precipitate was washed to remove the remaining aqueous salts and dried overnight in a convection oven at  $95^\circ\text{C}$ . Alkali-promoted catalysts containing either lithium, sodium, or potassium were prepared through wet impregnation of manganese molybdate with the alkali carbonate and again dried overnight in a convection oven at  $95^\circ\text{C}$ . The pure manganese molybdate and the alkali-promoted catalysts were calcined in oxygen for 4 h at  $800^\circ\text{C}$ . These catalysts have been characterized through a number of techniques including BET surface area using krypton as the adsorbate (Micromeritics 2100E Accusorb), X-ray diffraction (Scintag PAD V diffractometer with  $\text{Cu K}_\alpha$  radiation), X-ray photoelectron spectroscopy (Physical Electronics/Perkin Elmer, model 550), laser Raman spectroscopy (Spex Triplemate 1877) using a CCD (couple charged device) detector, temperature programmed studies, and oxygen exchange using isotopically labeled oxygen.

A quartz fixed-bed reactor with 9 mm o.d. and 5 mm i.d. was used for the catalytic reaction experiments. The diameter was reduced to 2 mm at the end of the catalyst bed to allow rapid exiting of the gas stream. The isothermal portion of the quartz tube was determined to be 20 mm. The catalyst bed length ranged from 8 to 11 mm, with a quartz wool plug inserted to hold the bed in place. The total surface

area used for each catalyst was  $0.1\text{ m}^2$ . Blank studies using an empty reactor, or a reactor filled with quartz chips, revealed the homogeneous reaction under the experimental conditions to produce small amounts of ethane and formaldehyde with no quantifiable formation of CO or  $\text{CO}_2$ . The reaction feed gas consisted of methane, oxygen and nitrogen or helium (ratio = 2 : 1 : 3) with a total flow rate of  $9.3\text{ cm}^3(\text{STP})/\text{min}$ . The feed gas composition was maintained using mass flow controllers (Tylan). Helium was used as the diluent for the isotopic studies, while nitrogen was used as the diluent for product quantification by gas chromatography. Product stream compositions were determined using an automated HP 5890 gas chromatograph.  $\text{CH}_4$ ,  $\text{CO}_2$ , CO,  $\text{N}_2$ ,  $\text{O}_2$ , HCHO, and  $\text{C}_2$  hydrocarbons were separated and analyzed by a thermal conductivity detector using an Haysep T column connected to a molecular sieve 5A column through an isolation valve. Coupling products were also separated and analyzed through a second Haysep T column connected to a flame ionization detector.

The setup used for the isotopic labeling experiments with  $^{13}\text{CH}_4$  was also used previously for isotopic labeling experiments with  $^{18}\text{O}_2$  [11]. The isotopic experiments utilized a four-port Valco valve in the gas flow stream to switch the methane feed gas source from  $^{12}\text{CH}_4$  (Matheson) to  $^{13}\text{CH}_4$  (Isotec, 99 at%  $^{13}\text{C}$ ). The isotopic transients were obtained under steady-state conditions after approximately 15 h of reaction. The reaction gas composition was continuously monitored during the isotopic experiments by a quadrupole mass spectrometer (HP 5989A MS engine) and the transients for methane, CO, and  $\text{CO}_2$  were obtained through continuous monitoring. Because of the difficulty in detecting ethane and ethylene in continuous mode, isotopic labeling experiments were repeated by sending pulses of the effluent gas through the gas chromatograph before entering the mass spectrometer. The pulses were taken with 30 s intervals and separation of the species was achieved by using a Poraplot Q column. The gas-phase holdup was measured separately by switching from an argon/oxygen/helium stream to the methane/oxygen/helium stream and following the decay of the argon signal. The gas-phase holdup measurements were also repeated using both the continuous detection mode and pulse detection mode. Due to system modifications required for the experiments to be run in the pulse detection mode, the gas-phase holdup time for this set of experiments was substantially longer than for the experiments run in the continuous detection mode.

### 3. Results and discussion

#### 3.1. CHARACTERIZATION STUDIES

As typically occurs when alkali promoters are used, we observed a decrease in the promoted catalyst surface area from that of pure manganese molybdate. Our characterization studies revealed no major changes in the crystal structure from

unpromoted manganese molybdate due to the addition of any of the promoter ions. The X-ray diffraction patterns and Raman spectra showed the molybdate structure to be intact with only minor changes in the relative band intensities. Further details of the characterization results are reported elsewhere [1,11].

### 3.2. STEADY-STATE REACTION STUDIES

The results from the gas chromatographic analysis of the products are presented in table 1. The experiments were performed using catalyst amounts based on equal surface area ( $0.1 \text{ m}^2$ ), so the bed length was different for each catalyst. However, the trends observed were the same as those found during previous studies when both the bed length and the surface area were held constant [1]. In each case the addition of the promoter ion to  $\text{MnMoO}_4$  increased the catalytic formation of coupling or partial oxidation products. The highest activity was observed over the Na-promoted catalyst, but the most selective catalyst for  $\text{C}_2$  hydrocarbons formation was the K-promoted catalyst. The increased selectivity of the K-promoted catalyst was found to be even more striking when these catalysts were compared previously at equal conversion levels [1]. When the conversion level was kept at 10% for all catalysts, a selectivity of 41% to  $\text{C}_2$  hydrocarbons was obtained for the K-promoted catalyst as compared to 1, 3, and 10% for the unpromoted  $\text{MnMoO}_4$ , and the  $\text{MnMoO}_4$  catalysts promoted with Li and Na, respectively.

### 3.3. $^{12}\text{CH}_4/^{13}\text{CH}_4$ ISOTOPIC LABELING STUDIES

The results from the gas-phase holdup measurements for the experiments run in the continuous detection mode are shown in fig. 1. The argon decay curves show no variation in gas-phase holdup for different catalyst beds.

The  $^{12}\text{C}$  transient results from the isotopic labeling studies are plotted as normalized isotope concentrations versus time. The mass spectrometer signals for the labeled and unlabeled species of each compound were obtained, with the relative signal intensity used to calculate the concentrations. The concentrations are plotted on a scale of 0 to 1.0 where 1.0 represents 100%  $^{12}\text{C}$  content.

The transients for  $^{12}\text{CH}_4$ ,  $^{12}\text{CO}$ , and  $^{12}\text{CO}_2$  are plotted for each catalyst in fig. 2 for comparison of the relative decay times of the unlabeled species. The tran-

Table 1  
Conversion and production rates ( $\mu\text{mol}/\text{m}^2 \text{ min}$ )

| Catalyst                   | SA<br>( $\text{m}^2/\text{g}$ ) | $\text{CH}_4$ | $\text{CO}$ | $\text{CO}_2$ | $\text{HCHO}$ | $\text{C}_2$ | % selectivity<br>to $\text{C}_2$ |
|----------------------------|---------------------------------|---------------|-------------|---------------|---------------|--------------|----------------------------------|
| $\text{MnMoO}_4$           | 0.46                            | 50            | 24          | 15            | 10            | 0.6          | 2.2                              |
| $\text{Li}/\text{MnMoO}_4$ | 0.30                            | 108           | 48          | 38            | 20            | 2.1          | 3.8                              |
| $\text{Na}/\text{MnMoO}_4$ | 0.19                            | 128           | 56          | 43            | 23            | 5.7          | 8.5                              |
| $\text{K}/\text{MnMoO}_4$  | 0.29                            | 55            | 14          | 25            | 11            | 4.5          | 15.6                             |

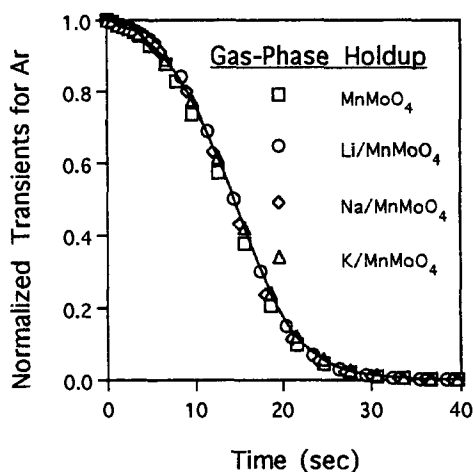


Fig. 1. Gas-phase holdup measurements using Ar.

sients for the unpromoted and Li- and Na-promoted catalysts are plotted out to 40 s, while the transients for the K-promoted catalyst are plotted out further to 120 s. The most pronounced difference is observed over K/MnMoO<sub>4</sub> catalyst in that the  $^{12}\text{CO}$  decay almost levels off at around 20% and remains non-zero even after 120 s following the isotopic switch. The  $^{12}\text{CO}_2$  decay curve, on the other hand, shows a similar residence time as that observed for the other catalysts studied.

The C<sub>2</sub> hydrocarbon and formaldehyde transients were not possible to obtain from the data for any of the catalysts; the mass spectrometer signals representing the decay of these compounds could not accurately be followed in continuous monitoring mode. To compensate for this problem, experiments were repeated where pulses of the effluent stream were passed through a gas chromatograph before entering the mass spectrometer. This method combined by the selective ion monitoring technique allowed accurate detection of ethane and ethylene. For this set of experiments, the signals for CH<sub>4</sub>, CO<sub>2</sub>, C<sub>2</sub>H<sub>6</sub>, and C<sub>2</sub>H<sub>4</sub> were monitored. The gas-phase holdup measurements were also repeated using the pulse detection mode. When the feed stream was switched from an Ar–He mixture to a mixture of O<sub>2</sub>–He, the Ar signal was seen to drop to zero by the third pulse. The normalized isotope concentrations measured with 30 s intervals are presented in fig. 3. As seen in the figure, both methane and carbon dioxide transients decay to zero by the third pulse, whereas ethane and ethylene transients remain at a non-zero value. It should be noted that in these experiments the reactor is maintained under continuous flow and steady-state conditions. It is only the monitoring of the isotope composition of the effluent stream which is performed in the pulse mode.

As shown by the argon transients indicating the gas-phase holdup, after 30 s in the continuous detection mode and after the third pulse in the pulse detection mode following the switch from  $^{12}\text{CH}_4$  to  $^{13}\text{CH}_4$ , the catalyst surface becomes the sole

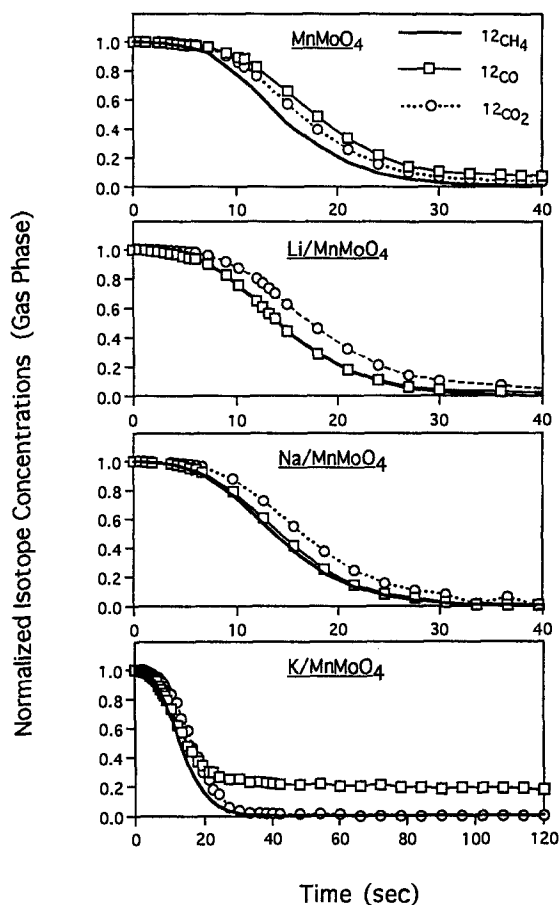


Fig. 2.  $^{12}\text{C}$  transients for  $\text{CH}_4$ ,  $\text{CO}$ , and  $\text{CO}_2$  obtaining using continuous monitoring of the effluent stream.

source of unlabeled carbon for either desorption as  $^{12}\text{CH}_4$ , or reaction to form unlabeled products. Coking was not observed under the reaction conditions, either on the reactor walls or on used catalyst surfaces. Methane was found to quickly decay in  $^{12}\text{C}$  content during the gas-phase holdup time, and within experimental error, no  $^{12}\text{C}$  labeled methane molecules were later detected. The short residence time of methane on the surface could indicate weak interaction, or irreversible adsorption leading to further reaction.

The unlabeled carbon monoxide rapidly disappears for the Li- and Na-promoted  $\text{MnMoO}_4$  catalysts, but does remain longer on the catalyst surface for unpromoted and K-promoted  $\text{MnMoO}_4$  catalyst. The longer residence time of carbon monoxide for these catalysts may indicate a multi-step reaction, strong adsorption, or readsorption of the product or a longer residence time for a species which is a precursor for carbon monoxide. To determine which one of these possibilities

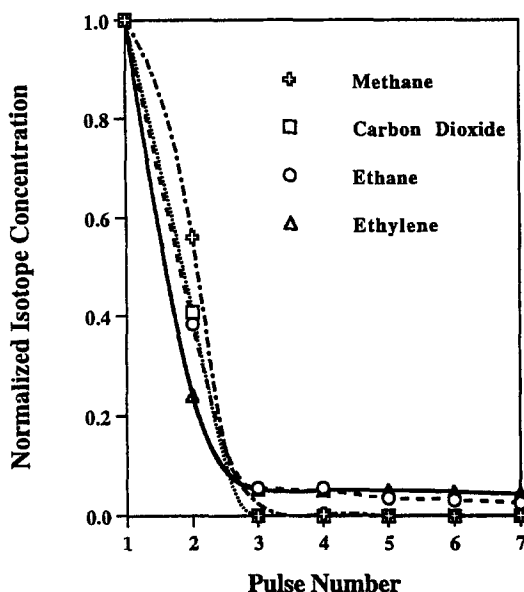


Fig. 3.  $^{12}\text{C}$  transients for  $\text{CH}_4$ ,  $\text{CO}_2$ , ethane and ethylene obtained using pulsed monitoring of the effluent stream

would explain the observed data better, we ran a series of experiments where pulses of Ar, CO, and  $\text{CO}_2$  were passed over the catalyst at reaction conditions. The results showed no difference in the length of time that it took for these species to go through the system. These experiments indicated that it is not the interaction of the final products, i.e., CO and  $\text{CO}_2$  with the surface that leads to a slower decay behavior for CO, but the surface residence of another species which could be a precursor to CO.

The experiments performed to monitor the transients for ethane and ethylene provided the most interesting results in showing a non-zero signal for unlabeled ethane and ethylene for another 2 min after unlabeled methane was completely flushed out of the system while the unlabeled  $\text{CO}_2$  and methane signals decayed to zero within the time period that it takes for an inert species to exit the system.

Briefly summarizing results obtained in similar isotopic labeling studies using oxygen, changing the feed gas source from  $^{16}\text{O}_2$  to  $^{18}\text{O}_2$  under reaction conditions revealed a different interaction between gas-phase oxygen and the K/MnMoO<sub>4</sub> catalyst compared to the other catalysts studied. The  $^{16}\text{O}$  incorporation into products decreased for the K-promoted catalysts significantly faster as compared to the other catalysts studied, but the  $^{16}\text{O}$  incorporation into molecular oxygen remained greater. The  $^{16}\text{O}$  flux in the form of  $\text{CO}_2$  continued much longer than the residence time of the  $^{12}\text{CO}_2$  for all of the catalysts, showing that the detection of  $\text{CO}_2$  with unlabeled oxygen long after the  $^{16}\text{O}_2/^{18}\text{O}_2$  isotopic switch was not due to slow desorption of carbon dioxide from the surface or significant readsorption of

carbon dioxide by the catalyst, but was due to involvement of lattice oxygen in  $\text{CO}_2$  formation. In the case of  $\text{K/MnMoO}_4$  catalyst, however, the unlabeled oxygen incorporation into CO declined much more rapidly than for the other catalysts. Also worth noting was the fact that over  $\text{K/MnMoO}_4$ ,  $^{16}\text{O}$  incorporation into CO declined more rapidly than the  $^{16}\text{O}$  incorporation into  $\text{CO}_2$ , while all other catalysts showed the opposite trend. This observation, combined with the observation that  $^{12}\text{CO}$  signal did not decline to zero within the gas-phase hold-up time over  $\text{K/MnMoO}_4$ , leads us to suggest that methyl radicals have a longer "surface-life" over  $\text{K/MnMoO}_4$  and that CO, in part, is formed from the methyl radicals. The longer surface residency of methyl radicals, on the other hand, could allow for the desorption and subsequent coupling of these species into  $\text{C}_2$  hydrocarbons, leading to higher  $\text{C}_2$  selectivity. The fact that the unlabeled ethane and ethylene signals remained at a non-zero value while the unlabeled methane and  $\text{CO}_2$  signals decayed to zero within the gas-phase holdup time also supports our suggestion that  $\text{C}_2$  formation is possible if methyl radicals can remain on the surface long enough without rapidly being oxidized to carbon dioxide. It is also conceivable that, over  $\text{K/MnMoO}_4$ , gas phase oxygen plays a bigger role in CO formation through oxidation of the desorbed methyl radicals than it does over the other catalysts. The differences in the residence times of CO and  $\text{CO}_2$  on the K-promoted catalyst indicates that  $\text{CO}_2$  formation could take place through multiple pathways, including direct oxidation of methane.

Another significant piece of information obtained from our isotopic labeling studies using  $^{18}\text{O}_2$  was the formation of virtually 100%  $\text{H}_2^{16}\text{O}$  for the Li- and Na-promoted catalysts over a 15 min time period as compared to increasing incorporation of  $^{18}\text{O}$  by the unpromoted and K-promoted  $\text{MnMoO}_4$ . This not only indicates that the formation of water over Li- and Na-promoted catalysts takes place almost exclusively through the incorporation of lattice oxygen, but also implies a rapid diffusion of oxygen from the bulk to the surface. The shorter residence time of  $^{12}\text{CO}$  on these catalysts may also indicate that they have a higher activity for oxidizing the methyl radical, once it is formed, rather than allowing it to stay on the surface and to desorb subsequently.

$\text{MnMoO}_4$  and alkali-promoted  $\text{MnMoO}_4$  catalysts exhibit significantly different behaviors in the catalytic steps that lead to coupling or complete oxidation of methane. The unpromoted and K-promoted  $\text{MnMoO}_4$  catalysts show lower catalytic activity as compared to the Li- or Na-promoted catalysts, accompanied by a longer "apparent" residence time of carbon monoxide. The persisting non-zero signal observed for unlabeled ethane and ethylene suggests that the sites which provide a longer "surface life" for methyl radicals are the controlling factors for increased  $\text{C}_2$  selectivity. This observation combined with the increased selectivity of the K-promoted catalyst for  $\text{C}_2$  species implies that these sites, which appear to be associated with the formation/retention of methyl radicals, could be attributed to the presence of K-promoter ions on the surface of the catalyst. The higher activity and the lower selectivity of the Li- and Na-promoted  $\text{MnMoO}_4$  catalysts, on



the other hand, could be attributed to the availability of highly active oxygen species on the surface, which may readily oxidize the methyl radicals. The presence of highly active surface oxygen species can be explained by the formation of defect sites, which may lead to increased mobility of the lattice oxygen, due to the incorporation of the Li and Na promoter ions into the molybdate structure.

## Acknowledgement

The financial support provided by the National Science Foundation through Grant CTS-8912247 is gratefully acknowledged.

## References

- [1] S.A. Driscoll, L. Zhang and U.S. Ozkan, in: *Catalytic Selective Oxidation*, Vol. 523, eds. S.T. Oyama and J.W. Hightower (American Chemical Society, Washington, 1993) p. 340.
- [2] G.E. Keller and M.M. Bhasin, *J. Catal.* 73 (1982) 9.
- [3] T. Ito and J.H. Lunsford, *Nature* 314 (1985) 721.
- [4] D.J. Driscoll, W. Martir, J.X. Wang and J.H. Lunsford, *J. Am. Chem. Soc.* 107 (1985) 58.
- [5] J.H. Lunsford, M.D. Cisneros, P.G. Hinson, Y. Tong and H. Zhang, *Faraday Discussions Chem. Soc.* 87 (1989) 13.
- [6] G.W. Keulks and M. Yu, in: *New Developments in Selective Oxidation*, eds. G. Centi and F. Trifirò (Elsevier, Amsterdam, 1990) p. 427.
- [7] C. Shi, M. Xu, M.P. Rosynek and J.H. Lunsford, *J. Phys. Chem.* 97 (1993) 216.
- [8] M. Hatano and J. Otsuka, *J. Chem. Soc. Faraday Trans. I* 85 (1989) 199.
- [9] C. Mirodatos, A. Holmen, R. Mariscal and G.A. Martin, *Catal. Today* 6 (1990) 601.
- [10] C. Mirodatos, V. Ducarme, H. Mozzanega, A. Holmen, J. Sanches-Marcano and Q. Wu, in: *Natural Gas Conversion*, eds. A. Holmen et al. (Elsevier, Amsterdam, 1991) p. 41.
- [11] S.A. Driscoll and U.S. Ozkan, *J. Phys. Chem.* 97 (44) (1993) 11524.
- [12] K.P. Peil, J.G. Goodwin Jr. and G.J. Marcelin, *J. Am. Chem. Soc.* 112 (1990) 6129.
- [13] K.P. Peil, J.G. Goodwin Jr. and G.J. Marcelin, *J. Phys. Chem.* 93 (1989) 5977.
- [14] K.P. Peil, J.G. Goodwin Jr. and G.J. Marcelin, *J. Catal.* 131 (1991) 143.
- [15] K.P. Peil, J.G. Goodwin Jr. and G.J. Marcelin, *J. Catal.* 132 (1991) 556.
- [16] K.P. Peil, J.G. Goodwin Jr. and G.J. Marcelin, in: *Natural Gas Conversion*, eds. A. Holmen et al. (Elsevier, Amsterdam, 1991) p. 73.
- [17] A. Ekstrom and J.A. Lapszewicz, *J. Am. Chem. Soc.* 111 (1989) 8515.
- [18] A. Ekstrom and J.A. Lapszewicz, *J. Phys. Chem.* 93 (1989) 5230.
- [19] I. Matsuura and M. Kirishiki, *Chem. Lett.* (1986) 1441.
- [20] N.W. Cant, C.A. Lukey and P.F. Nelson, *J. Catal.* 124 (1990) 336.
- [21] J. Rasko, G.A. Somorjai and H. Heinemann, *Appl. Catal. A* 84 (1992) 57.
- [22] S.A. Driscoll, D. Gardner and U.S. Ozkan, *J. Catal.*, accepted.